

Neutron skin thickness of ^{208}Pb determined from reaction cross section for proton scattering

Shingo Tagami, Tomotsugu Wakasa, Jun Matsui, and Masanobu Yahiro*
Department of Physics, Kyushu University, Fukuoka 819-0395, Japan

Maya Takechi
Niigata University, Niigata 950-2181, Japan
(Dated: June 1, 2021)

Background: The reaction cross section σ_R is useful to determine the neutron radius R_n as well as the matter radius R_m . The chiral (Kyushu) g -matrix folding model for ^{12}C scattering on ^9Be , ^{12}C , ^{27}Al targets was tested in the incident energy range of $30 \leq E_{\text{in}} \leq 400$ MeV, and it is found that the model reliably reproduces the σ_R in $30 \leq E_{\text{in}} \leq 100$ MeV and $250 \leq E_{\text{in}} \leq 400$ MeV.

Aim: We determine R_n and the neutron skin thickness R_{skin} of ^{208}Pb by using high-quality σ_R data for the $p + ^{208}\text{Pb}$ scattering in $30 \leq E_{\text{in}} \leq 100$ MeV. The theoretical model is the Kyushu g -matrix folding model with the densities calculated with Gongny-D1S HFB (GHFB) with the angular momentum projection (AMP).

Results: The Kyushu g -matrix folding model with the GHFB+AMP densities underestimates σ_R in $30 \leq E_{\text{in}} \leq 100$ MeV only by a factor of 0.97. Since the proton radius R_p calculated with GHFB+AMP agrees with the precise experimental data of 5.444 fm, the small deviation of the theoretical result from the data on σ_R allows us to scale the GHFB+AMP neutron density so as to reproduce the σ_R data. In $E_{\text{in}} = 30\text{--}100$ MeV, the experimental σ_R data can be reproduced by assuming the neutron radius of ^{208}Pb as $R_n = 5.722 \pm 0.035$ fm.

Conclusion: The present result $R_{\text{skin}} = 0.278 \pm 0.035$ fm is in good agreement with the recent PREX-II result of $r_{\text{skin}} = 0.283 \pm 0.071$ fm.

I. INTRODUCTION

Horowitz *et al.* [1] proposed a direct measurement for neutron skin $R_{\text{skin}} = R_n - R_p$, where $R_n \equiv \langle r_n^2 \rangle^{1/2}$ and $R_p \equiv \langle r_p^2 \rangle^{1/2}$ are the root-mean-square (rms) radii of point neutrons and protons, respectively. The measurement consists of parity-violating (PV) and elastic electron scattering. The neutron radius R_n is determined from the former experiment, whereas the proton radius R_p is from the latter.

Very recently, by combining the original Lead Radius Experiment (PREX) result [2, 3] with the updated PREX-II result, the PREX collaboration reported the following value [4]:

$$R_{\text{skin}}^{PV} = 0.283 \pm 0.071 \text{ fm}, \quad (1)$$

where the quoted uncertainty represents a 1σ error and has been greatly reduced from the original value of ± 0.177 fm (quadratic sum of experimental and model uncertainties) [3]. The R_{skin}^{PV} value is most reliable at the present stage, and provides crucial tests for the equation of state (EoS) of nuclear matter [5–9] as well as nuclear structure models. For example, Reed *et al.* [10] report a value of the sloop parameter L of the EoS and examine the impact of such a stiff symmetry energy on some critical neutron-star observables. It should be noted that the R_{skin}^{PV} value is considerably larger than the other experimental values which are significantly model dependent [11–14]. As an exceptional case, a nonlocal dispersive-optical-model (DOM) analysis of ^{208}Pb deduces $r_{\text{skin}}^{\text{DOM}} = 0.25 \pm 0.05$ fm [15], which is consistent with R_{skin}^{PV} . It is the aim of this paper to present the R_{skin} value with a similar precision of R_{skin}^{PV} by analyzing the reaction cross section σ_R for $p + ^{208}\text{Pb}$.

The reaction cross section σ_R is a powerful tool to determine matter radius R_m . One can evaluate R_{skin} and R_n by using the R_m and the R_p [16] determined by the electron scattering. The g -matrix folding model is a standard way of deriving microscopic optical potential for not only proton scattering but also nucleus-nucleus scattering [17–27]. Applying the folding model with the Melbourne g -matrix [20] for interaction cross sections σ_I for Ne isotopes and σ_R for Mg isotopes, we discovered that ^{31}Ne is a halo nucleus with large deformation [27], and deduced the matter radii r_m for Ne isotopes [28] and for Mg isotopes [29]. The folding potential is nonlocal, but is localized with the method of Ref. [17]. The validity is shown in Ref. [30]. For proton scattering, the localized version of g -matrix folding model [31] yields the same results as the full folding g -matrix folding model of Ref. [20], as shown by comparing the results of Ref. [31] with those of Ref. [20].

Recently, Kohno [32] calculated the g -matrix for the symmetric nuclear matter, using the Brueckner-Hartree-Fock method with chiral 4th-order ($N^3\text{LO}$) nucleon-nucleon (NN) forces ($2NFs$) and 3rd-order (NNLO) three-nucleon forces ($3NFs$). He set $c_D = -2.5$ and $c_E = 0.25$ so that the energy per nucleon can become minimum at $\rho = \rho_0$; see Fig. 1 for c_D and c_E . Toyokawa *et al.* [25] localized the non-local chiral g -matrix into three-range Gaussian forms. using the localization method proposed by the Melbourne group [20, 33, 34]. The resulting local g -matrix is called “Kyushu g -matrix”.

The Kyushu g -matrix folding model is successful in reproducing σ_R and differential cross sections $d\sigma/d\Omega$ for ^4He scattering in $E_{\text{in}} = 30\text{--}200$ MeV/nucleon [25]. The success is true for proton scattering at $E_{\text{in}} = 65$ MeV [23]. Lately, we predicted neutron skin r_{skin} and proton, neutron, matter radii, R_p , R_n , R_m from interaction cross sections σ_I ($\approx \sigma_R$) for $^{42-51}\text{Ca} + ^{12}\text{C}$ scattering at $E_{\text{in}} = 280$ MeV/nucleon, using the Kyushu g -matrix folding model with the densities calculated

* orion093g@gmail.com

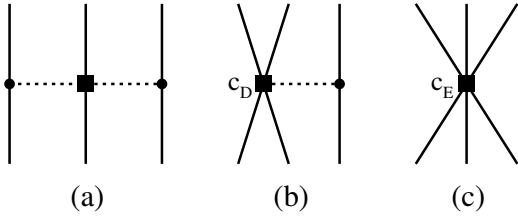


FIG. 1. 3NFs in NNLO. Diagram (a) corresponds to the Fujita-Miyazawa 2π -exchange 3NF [35], and diagrams (b) and (c) correspond to 1π -exchange and contact 3NFs. The solid and dashed lines denote nucleon and pion propagations, respectively, and filled circles and squares stand for vertices. The strength of the filled-square vertex is often called c_D in diagram (b) and c_E in diagram (c).

with Gogny-D1S HFB (GHFB) with and without the angular momentum projection (AMP) [26].

In Ref. [26], we tested the Kyushu g -matrix folding model for ^{12}C scattering on ^9Be , ^{12}C , ^{27}Al targets in $30 \lesssim E_{\text{in}} \lesssim 400$ MeV, comparing the theoretical σ_R with the experimental data [36]. We found that the Kyushu g -matrix folding model is reliable for σ_R in $30 \lesssim E_{\text{in}} \lesssim 100$ MeV and $250 \lesssim E_{\text{in}} \lesssim 400$ MeV. This indicates that the Kyushu g -matrix folding model is applicable in $30 \lesssim E_{\text{lab}} \lesssim 100$ MeV, although the data on $p + ^{208}\text{Pb}$ scattering are available in $21 \lesssim E_{\text{lab}} \lesssim 180$ MeV.

In this paper, we present the determination of $R_{\text{skin}}^{\text{GHFB}}$ from the measured σ_R for $p + ^{208}\text{Pb}$ scattering in $30 \lesssim E_{\text{in}} \lesssim 100$ MeV [37–39], using the Kyushu g -matrix folding model with the GHFB+AMP densities. As mentioned above, the Kyushu g -matrix folding model is applicable in $30 \lesssim E_{\text{in}} \lesssim 100$ MeV, although the data on $p + ^{208}\text{Pb}$ scattering are available in $21 \lesssim E_{\text{in}} \lesssim 180$ MeV. In Sec. II, we briefly describe our model. Section III presents the results and a comparison with $R_{\text{skin}}^{\text{PV}}$, and discussion follows. Finally, Sec. IV is devoted to a summary.

II. MODEL

Our model is the Kyushu g -matrix folding model [25] with the densities calculated with GHFB+AMP [26]. In Ref. [25], the Kyushu g -matrix is constructed from chiral interaction with the cutoff $\Lambda = 550$ MeV. The model was tested for ^{12}C scattering on ^9Be , ^{12}C , and ^{27}Al targets in $30 \lesssim E_{\text{in}} \lesssim 400$ MeV. It is found that the Kyushu g -matrix folding model is good in $30 \lesssim E_{\text{in}} \lesssim 100$ MeV and $250 \lesssim E_{\text{in}} \lesssim 400$ MeV [26].

The brief formulation of the folding model itself is shown below. For nucleon-nucleus scattering, the potential is composed of the direct and exchange parts, U^{DR} and U^{EX} [29]:

$$U^{\text{DR}}(\mathbf{R}) = \sum_{\mu, \nu} \int \rho_{\text{T}}^{\nu}(\mathbf{r}_{\text{T}}) g_{\mu\nu}^{\text{DR}}(s; \rho_{\mu\nu}) d\mathbf{r}_{\text{T}}, \quad (2a)$$

$$U^{\text{EX}}(\mathbf{R}) = \sum_{\mu, \nu} \int \rho_{\text{T}}^{\nu}(\mathbf{r}_{\text{T}}, \mathbf{r}_{\text{T}} + \mathbf{s}) \times g_{\mu\nu}^{\text{EX}}(s; \rho_{\mu\nu}) \exp[-i\mathbf{K}(\mathbf{R}) \cdot \mathbf{s}/M] d\mathbf{r}_{\text{T}} \quad (2b)$$

where \mathbf{R} is the relative coordinate between a projectile (P) and a target (T), $\mathbf{s} = -\mathbf{r}_{\text{T}} + \mathbf{R}$, and \mathbf{r}_{T} is the coordinate of the interacting nucleon from T. Each of μ and ν denotes the z -component of isospin; $1/2$ means neutron and $-1/2$ does proton. The nonlocal U^{EX} has been localized in Eq. (2b) with the local semi-classical approximation [17], where $\mathbf{K}(\mathbf{R})$ is the local momentum between P and T, and $M = A/(1+A)$ for the target mass number A ; see Ref. [30] for the validity of the localization. The direct and exchange parts, $g_{\mu\nu}^{\text{DR}}$ and $g_{\mu\nu}^{\text{EX}}$, of the g -matrix depend on the local density

$$\rho_{\mu\nu} = \rho_{\text{T}}^{\nu}(\mathbf{r}_{\text{T}} + \mathbf{s}/2), \quad (3)$$

at the midpoint of the interacting nucleon pair; see Ref. [28] for the explicit forms of $g_{\mu\nu}^{\text{DR}}$ and $g_{\mu\nu}^{\text{EX}}$.

The relative wave function ψ is decomposed into partial waves χ_L , each with different orbital angular momentum L . The elastic S -matrix elements S_L are obtained from the asymptotic form of the χ_L . The total reaction cross section σ_R is calculable from the S_L as

$$\sigma_R = \frac{\pi}{K^2} \sum_L (2L+1)(1 - |S_L|^2). \quad (4)$$

The proton and neutron densities, $\rho_p(r)$ and $\rho_n(r)$, are calculated with GHFB+AMP. As a way of taking the center-of-mass correction to the densities, we use the method of Ref. [28], since the procedure is quite simple.

III. RESULTS

Figure 2 shows the proton ρ_p^{GHFB} , neutron ρ_n^{GHFB} , and matter $\rho_m^{\text{GHFB}} \equiv \rho_p^{\text{GHFB}} + \rho_n^{\text{GHFB}}$ densities as a function of r . The experimental point-proton distribution extracted from the electron scattering data is also shown. The theoretical proton distribution ρ_p^{GHFB} reproduces the experimental ρ_p^{exp} reasonably well.

The Kyushu g -matrix folding model with the GHFB+AMP densities underestimates the σ_R data in $30 \lesssim E_{\text{in}} \lesssim 100$ MeV only by a factor of 0.97, as shown in Fig. 3. The proton radius $R_p^{\text{GHFB}} = 5.444$ fm calculated with GHFB+AMP agrees with the experimental value of $R_p^{\text{exp}} = 5.444$ fm [42]. Because of $\sigma_R \propto R_m^2$, the observed discrepancy of σ_R is attributed to the underestimation of ρ_m^{GHFB} originating from the underestimation of ρ_n^{GHFB} . Small deviation makes it possible to scale the GHFB+AMP densities for the neutron density so as to reproduce σ_R^{exp} in $E_{\text{in}} = 30$ – 100 MeV. The result of the scaling is $R_n^{\text{exp}} = 5.722 \pm 0.035$ fm leading to

$$R_{\text{skin}}^{\text{exp}} = 0.278 \pm 0.035 \text{ fm}. \quad (5)$$

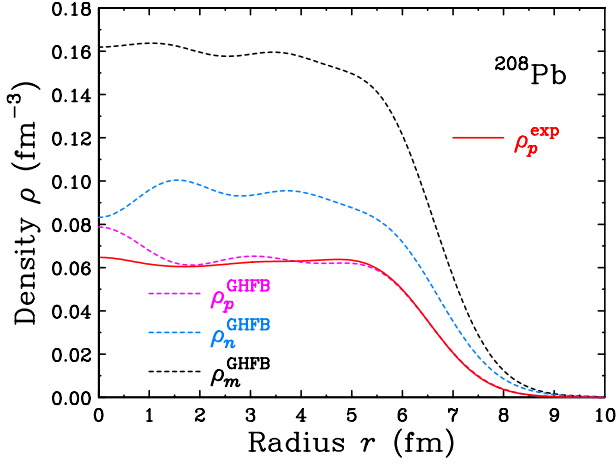


FIG. 2. r dependence of densities, $\rho_p(r)$, $\rho_n(r)$, $\rho_m(r)$, for ^{208}Pb calculated with GHFB+AMP. Three dashed lines from the bottom to the top denote $\rho_p(r)$, $\rho_n(r)$, $\rho_m(r)$, respectively. The experimental point-proton (unfolded) density ρ_p is taken from Refs. [40, 41].

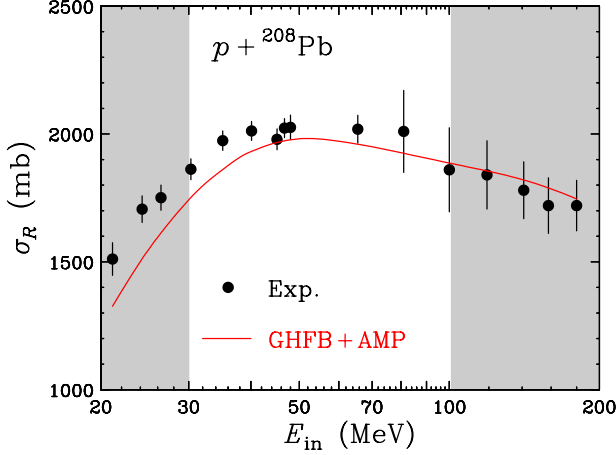


FIG. 3. E_{in} dependence of reaction cross sections σ_R for $p+^{208}\text{Pb}$ scattering. The solid line stands for the results of the Kyushu g -matrix folding model with GHFB+AMP densities. The data are taken from Refs. [37–39].

This result is consistent with $R_{\text{skin}}^{PV} = 0.283 \pm 0.071$ fm.

Now we show a simple derivation of R_n^{exp} in the limit of $K^{\text{exp}} = K^{\text{th}}$. The experimental and theoretical (GHFB+AMP) reaction cross sections, σ_R^{exp} and σ_R^{th} , can be expressed as

$$\sigma_R^{\text{exp}} = K^{\text{exp}} \left[(R_p^{\text{exp}})^2 \frac{Z}{A} + (R_n^{\text{exp}})^2 \frac{N}{A} \right], \quad (6a)$$

$$\sigma_R^{\text{th}} = K^{\text{th}} \left[(R_p^{\text{th}})^2 \frac{Z}{A} + (R_n^{\text{th}})^2 \frac{N}{A} \right], \quad (6b)$$

where Z , N , and A are proton, neutron, and atomic numbers of ^{208}Pb , respectively, and K is a proportional coefficient between σ_R and $R_m^2 = R_p^2(Z/A) + R_n^2(N/A)$. By using $K^{\text{exp}} = K^{\text{th}}$ and $R_p^{\text{exp}} = R_p^{\text{th}}$, the experimental neutron

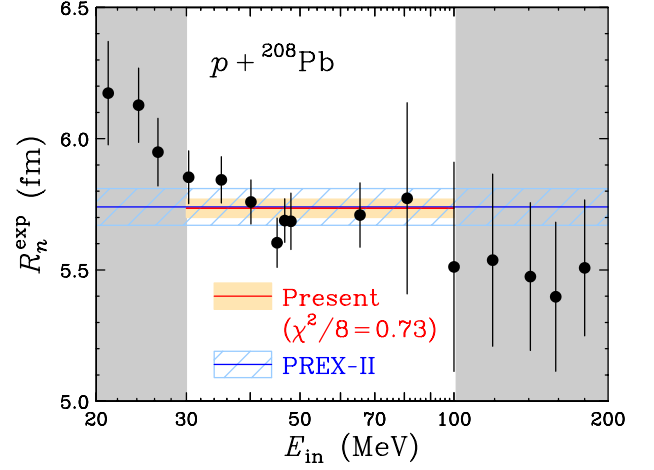


FIG. 4. Neutron radius R_n^{exp} of ^{208}Pb deduced from the $p+^{208}\text{Pb}$ reaction cross section and the theoretical Kyushu g -matrix folding model calculations as a function of incident energy E_{in} .

radius R_n^{exp} can be deduced as

$$R_n^{\text{exp}} = \sqrt{\frac{Z(R_p^{\text{exp}})^2 + N(R_n^{\text{th}})^2}{N\sigma_R^{\text{th}}} \sigma_R^{\text{exp}} - (\sigma_p^{\text{exp}})^2 \frac{Z}{N}}, \quad (7)$$

from the experimental σ_R^{exp} and R_p^{exp} data and the theoretical R_n^{th} in GHFB+AMP.

Figure 4 shows the R_n^{exp} results as a function of incident energy E_{in} . The deduced R_n^{exp} values are almost independent of E_{in} in the region of $E_{\text{in}} = 30\text{--}100$ MeV where the present folding model is reliable [26]. By combining the eight data in this energy region, the neutron radius of ^{208}Pb becomes $\bar{R}_n^{\text{exp}} = 5.735 \pm 0.035$ fm as shown by the filled band in Fig. 4. This result shows that the neutron skin thickness of ^{208}Pb is $R_n^{\text{exp}} = 0.291 \pm 0.035$ fm with $R_p^{\text{exp}} = 5.444$ fm [42]. The limit of $K^{\text{exp}} = K^{\text{th}}$ is thus good, since $R_n^{\text{exp}} = 0.291 \pm 0.035$ fm is close to Eq.(5). Equation (7) is quite useful when $\sigma_R^{\text{exp}} \approx \sigma_R^{\text{th}}$ and $R_p^{\text{exp}} \approx R_p^{\text{th}}$.

IV. SUMMARY

The proton radius R_p calculated with GHFB+AMP agrees with the precise experimental data of 5.444 fm. In $30 \leq E_{\text{in}} \leq 100$ MeV, we can obtain r_n^{exp} from σ_R^{exp} by scaling the GHFB+AMP neutron density so as to reproduce σ_R^{exp} for each E_{in} , and take the weighted mean and its error for the resulting r_n^{exp} . From the resulting $R_n^{\text{exp}} = 5.722 \pm 0.035$ fm and $r_n^{\text{exp}} = 5.444$ fm, we can get $R_{\text{skin}}^{\text{exp}} = 0.278 \pm 0.035$ fm.

In conclusion, our result $R_{\text{skin}}^{\text{exp}} = 0.278 \pm 0.035$ fm is consistent with a new result r_{skin}^{208} (PREX II) = 0.283 ± 0.071 fm of PREX-II.

ACKNOWLEDGMENTS

We would like to thank Dr. Toyokawa for providing his code.

-
- [1] C. J. Horowitz, S. J. Pollock, P. A. Souder, and R. Michaels, *Phys. Rev. C* **63**, 025501 (2001).
- [2] S. Abrahamyan, Z. Ahmed, H. Albataineh, K. Aniol, D. S. Armstrong, W. Armstrong, T. Averett, B. Babineau, A. Barbieri, V. Bellini, *et al.* (PREX Collaboration), *Phys. Rev. Lett.* **108**, 112502 (2012).
- [3] C. J. Horowitz, Z. Ahmed, C.-M. Jen, A. Rakhman, P. A. Souder, M. M. Dalton, N. Liyanage, K. D. Paschke, K. Saenboonruang, R. Silwal, G. B. Franklin, M. Friend, B. Quinn, K. S. Kumar, D. McNulty, L. Mercado, S. Riordan, J. Wexler, R. W. Michaels, and G. M. Urciuoli, *Phys. Rev. C* **85**, 032501 (2012).
- [4] D. Adhikari, H. Albataineh, D. Androic, K. Aniol, D. S. Armstrong, T. Averett, S. Barcus, V. Bellini, R. S. Beminiwatta, J. F. Benesch, *et al.*, arXiv:2102.10767 [nucl-ex].
- [5] S. J. Novario, G. Hagen, G. R. Jansen, and T. Papenbrock, *Phys. Rev. C* **102**, 051303 (2020).
- [6] H. Shen, F. Ji, J. Hu, and K. Sumiyoshi, *Astrophys. J.* **891**, 148 (2020).
- [7] C. Horowitz, *Ann. Phys. (Amsterdam)* **411**, 167992 (2019).
- [8] Wei, Jin-Biao, Lu, Jia-Jing, Burgio, G. F., Li, Zeng-Hua, and Schulze, H.-J., *Eur. Phys. J. A* **56**, 63 (2020).
- [9] M. Thiel, C. Sfienti, J. Piekarewicz, C. J. Horowitz, and M. Vanderhaeghen, *J. Phys. G: Nucl. Part. Phys.* **46**, 093003 (2019).
- [10] B. T. Reed, F. J. Fattoyev, C. J. Horowitz, and J. Piekarewicz, arXiv:2101.03193 [nucl-th].
- [11] A. Trzcńska, J. Jastrzębski, P. Lubiński, F. J. Hartmann, R. Schmidt, T. von Egidy, and B. Klos, *Phys. Rev. Lett.* **87**, 082501 (2001).
- [12] J. Zenihiro, H. Sakaguchi, T. Murakami, M. Yosoi, Y. Yasuda, S. Terashima, Y. Iwao, *et al.*, *Phys. Rev. C* **82**, 044611 (2010).
- [13] A. Tamii, I. Poltoratska, P. von Neumann-Cosel, Y. Fujita, T. Adachi, C. A. Bertulani, J. Carter, *et al.*, *Phys. Rev. Lett.* **107**, 062502 (2011).
- [14] C. M. Tarbert, D. P. Watts, D. I. Glazier, P. Aguar, J. Ahrens, J. R. M. Annand, H. J. Arends, R. Beck, V. Bekrenev, B. Boilat, *et al.* (Crystal Ball at MAMI and A2 Collaboration), *Phys. Rev. Lett.* **112**, 242502 (2014).
- [15] M. C. Atkinson, M. H. Mahzoon, M. A. Keim, B. A. Bordelon, C. D. Pruitt, R. J. Charity, and W. H. Dickhoff, *Phys. Rev. C* **101**, 044303 (2020).
- [16] I. Angeli and K. Marinova, *At. Data Nucl. Data Tables* **99**, 69 (2013).
- [17] F. Brieva and J. Rook, *Nucl. Phys. A* **291**, 299 (1977); *Nucl. Phys. A* **291**, 317 (1977); *Nucl. Phys. A* **297**, 206 (1978).
- [18] G. Satchler and W. Love, *Physics Reports* **55**, 183 (1979); G. R. Satchler, *Direct Nuclear Reactions* (Oxford University Press, 1983).
- [19] N. Yamaguchi, S. Nagata, and T. Matsuda, *Prog. Theor. Phys.* **70**, 459 (1983); S. Nagata, M. Kamimura, and N. Yamaguchi, *Prog. Theor. Phys.* **73**, 512 (1985); N. Yamaguchi, S. Nagata, and J. Michiyama, *Prog. Theor. Phys.* **76**, 1289 (1986).
- [20] K. Amos, P. J. Dortmans, H. V. von Geramb, S. Karataglidis, and J. Raynall, “Nucleon-nucleus scattering: A microscopic nonrelativistic approach,” in *Advances in Nuclear Physics*, edited by J. W. Negele and E. Vogt (Springer US, Boston, MA, 2000) pp. 276–536.
- [21] T. Furumoto, Y. Sakuragi, and Y. Yamamoto, *Phys. Rev. C* **78**, 044610 (2008); *Phys. Rev. C* **79**, 011601 (2009); *Phys. Rev. C* **80**, 044614 (2009).
- [22] K. Egashira, K. Minomo, M. Toyokawa, T. Matsumoto, and M. Yahiro, *Phys. Rev. C* **89**, 064611 (2014).
- [23] M. Toyokawa, K. Minomo, M. Kohno, and M. Yahiro, *J. Phys. G: Nucl. Part. Phys.* **42**, 025104 (2014); *J. Phys. G: Nucl. Part. Phys.* **44**, 079502 (2017).
- [24] M. Toyokawa, M. Yahiro, T. Matsumoto, K. Minomo, K. Ogata, and M. Kohno, *Phys. Rev. C* **92**, 024618 (2015); *Phys. Rev. C* **96**, 059905(E) (2017).
- [25] M. Toyokawa, M. Yahiro, T. Matsumoto, and M. Kohno, *Prog. Theor. Exp. Phys.* **2018**, 023D03 (2018).
- [26] S. Tagami, M. Tanaka, M. Takechi, M. Fukuda, and M. Yahiro, *Phys. Rev. C* **101**, 014620 (2020).
- [27] K. Minomo, T. Sumi, M. Kimura, K. Ogata, Y. R. Shimizu, and M. Yahiro, *Phys. Rev. Lett.* **108**, 052503 (2012).
- [28] T. Sumi, K. Minomo, S. Tagami, M. Kimura, T. Matsumoto, K. Ogata, Y. R. Shimizu, and M. Yahiro, *Phys. Rev. C* **85**, 064613 (2012).
- [29] S. Watanabe, K. Minomo, M. Shimada, S. Tagami, M. Kimura, M. Takechi, M. Fukuda, D. Nishimura, T. Suzuki, T. Matsumoto, *et al.*, *Phys. Rev. C* **89**, 044610 (2014).
- [30] K. Minomo, K. Ogata, M. Kohno, Y. R. Shimizu, and M. Yahiro, *J. Phys. G: Nucl. Part. Phys.* **37**, 085011 (2010).
- [31] M. Toyokawa, K. Minomo, and M. Yahiro, *Phys. Rev. C* **88**, 054602 (2013).
- [32] M. Kohno, *Phys. Rev. C* **88**, 064005 (2013); *Phys. Rev. C* **96**, 059903(E) (2017).
- [33] H. V. von Geramb, K. Amos, L. Berge, S. Bräutigam, H. Kohlhoff, and A. Ingemarsson, *Phys. Rev. C* **44**, 73 (1991).
- [34] P. J. Dortmans and K. Amos, *Phys. Rev. C* **49**, 1309 (1994).
- [35] J. Fujita and H. Miyazawa, *Prog. Theor. Phys.* **17**, 360 (1957); *Prog. Theor. Phys.* **17**, 366 (1957).
- [36] M. Takechi, M. Fukuda, M. Mihara, K. Tanaka, T. Chinda, T. Matsumasa, M. Nishimoto, R. Matsumiya, Y. Nakashima, H. Matsubara, *et al.*, *Phys. Rev. C* **79**, 061601 (2009).
- [37] R. F. Carlson, A. J. Cox, J. R. Nimmo, N. E. Davison, S. A. Elbakk, J. L. Horton, A. Houdayer, A. M. Sourkes, W. T. H. van Oers, and D. J. Margaziotis, *Phys. Rev. C* **12**, 1167 (1975).
- [38] A. Ingemarsson, J. Nyberg, P. Renberg, O. Sundberg, R. Carlson, A. Auce, R. Johansson, G. Tibell, B. Clark, L. Kurth Kerr, and S. Hama, *Nucl. Phys. A* **653**, 341 (1999).
- [39] A. Auce, A. Ingemarsson, R. Johansson, M. Lantz, G. Tibell, R. F. Carlson, M. J. Shachno, A. A. Cowley, G. C. Hillhouse, N. M. Jacobs, *et al.*, *Phys. Rev. C* **71**, 064606 (2005).
- [40] H. De Vries, C. De Jager, and C. De Vries, *At. Data Nucl. Data Tables* **36**, 495 (1987).
- [41] H. Euteneuer, J. Friedrich, and N. Voegler,

Nucl. Phys. A **298**, 452 (1978).

[42] A. B. Jones and B. A. Brown, Phys. Rev. C **90**, 067304 (2014).